Four-phase computed tomography helps differentiation of renal oncocytoma with central hypodense areas from clear cell renal cell carcinoma

Jian-Yi Qu*
Hong Jiang*
Xin-Hong Song
Jin-Kun Wu
Heng Ma

*Jian-Yi Qu and Hong Jiang contributed equally to this work.

PURPOSE
To explore the utility of four-phase computed tomography (CT) in distinguishing renal oncocytoma with central hypodense areas from clear cell renal cell carcinoma (ccRCC).

METHODS
Eighteen patients with oncocytoma and 63 patients with ccRCC presenting with central hypodense areas were included in this study. All patients underwent four-phase CT imaging including the excretory phases later than 20 min after contrast injection. Two blinded experienced radiologists visually reviewed the enhancement features of the central hypodense areas in the excretory phase images and selected the area demonstrating the greatest degree of enhancement of the tumor in the corticomedullary phase images. Regions of interest (ROIs) were placed in the same location in each of the three contrast-enhanced imaging phases. Additionally, ROIs were placed in the adjacent normal renal cortex for normalization. The ratio of the lesion to cortex attenuation (L/C) for the three contrast-enhanced imaging phases and absolute de-enhancement were calculated. The receiver operating characteristic curve was used to obtain the cut-off values.

RESULTS
Complete enhancement inversion of the central areas was observed in 12 oncocytomas (66.67%) and 16 ccRCCs (25.40%) ($P = 0.003$). Complete enhancement inversion combined with L/C in the corticomedullary phase lower than 1.0 ($P < 0.001$) or absolute de-enhancement lower than 42.5 HU ($P < 0.001$) provided 86.42% and 85.19% accuracy, 61.11% and 55.56% sensitivity, 93.65% and 93.65% specificity, 73.33% and 71.43% positive predictive value (PPV), and 89.39% and 88.06% negative predictive value (NPV), respectively, for the diagnosis of oncocytomas. Combined with complete enhancement inversion, L/C in the corticomedullary phase lower than 1.0 and absolute de-enhancement lower than 42.5 HU provided 87.65%, 55.56%, 96.83%, 83.33%, and 88.41% of accuracy, sensitivity, specificity, PPV, and NPV, respectively, for the diagnosis of oncocytomas.

CONCLUSION
The combination of enhancement features of the central hypodense areas and the peripheral tumor parenchyma can help distinguish oncocytoma with central hypodense areas from ccRCC.

KEYWORDS
Cancer, MDCT, oncology, radiology, renal

From the Department of Radiology (J-Y.Q., H.J., X-H.S., H.M. ✉ mahengdoctor@163.com), Yantai Yuhuangding Hospital, Qingdao University School of Medicine, Yantai, China; Department of Pathology (J-K.W.), Yantai Yuhuangding Hospital, Qingdao University School of Medicine, Yantai, China.

Renal oncocytomas are virtually benign and account for 3%–7% of all renal tumors.[1] Based on the benign course and excellent prognosis of oncocytomas, partial nephrectomy and active surveillance are popular therapeutic options.[2] Accurate preoperative diagnosis is thus crucial. Although the features of oncocytoma shown on computed tomography (CT) and magnetic resonance imaging (MRI) have been extensively reported, these common imaging features have not been shown to accurately distinguished oncocytoma from

renal cell carcinoma (RCC), particularly from clear cell RCC (ccRCC), which is also a hypervascular tumor.[3-7]

Typical oncocytomas have previously been characterized by a central scar, which is seen in up to one-third of all cases.[8] However, this is not adequately specific, because the central scar is also present in three of the most common subtypes of RCC.[1] Moreover, the central necrotic areas within classic RCC can mimic a central scar; therefore, when central hypodense areas are observed on CT, they may indicate a central scar or necrosis. However, the contrast-enhanced CT features of the central scar within oncocytoma and the differences between oncocytoma and RCC central scar have not been studied in detail.

Several studies have focused on the differentiation of oncocytomas from ccRCCs on multiphase contrast-enhanced CT using different quantitative measures and enhancement correction methods.[4,5,9-14] However, these studies showed considerable overlap between oncocytomas and ccRCCs regarding their enhancement degree and pattern, making it difficult to confidently distinguish between them. In fact, many patients with benign renal tumors undergo unnecessary radical nephrectomy because the clinicians are unable to make an accurate preoperative diagnosis.

Different histopathologic structures of the central scar in oncocytomas and ccRCCs may lead to different appearances on CT; however, we hypothesized that if enhancement features of peripheral tumor parenchyma are also included, we can accurately distinguish typical oncocytoma with central scar from ccRCC.[1]

Therefore, we conducted this study to retrospectively explore whether oncocytomas with central hypodense areas can be differentiated from ccRCCs on four-phase CT based on enhancement features of the central hypodense areas and peripheral tumor parenchyma.

Methods

Patients

Our institutional review board approved the retrospective study (2019/298) and waived the requirement for informed consent owing to the retrospective nature of the study. We searched the radiology and pathology databases in our institution to identify all cases of histologically proven ccRCCs and oncocytomas between June 2013 and June 2019, in which all patients had undergone preoperative four-phase CT including the excretory phase later than 20 min after contrast injection. Two radiologists with three and five years of experience, respectively, reviewed all identified cases to select only tumors visually presenting central stellate or irregular hypodense areas compatible with central necrosis or scar in unenhanced or corticomedullary phase images. Cases without complete imaging or pathological data and central hypodense areas were excluded. In total, 81 patients and 81 tumors were included, of which 18 were oncocytomas and 63 were ccRCCs. Three patients each had two lesions (both of which were ccRCCs), but only one lesion in each patient was associated with central hypodensity.

CT examination

All CT examinations were performed using Philips Brilliance 64or 256 detector row helical scanners (Philips Healthcare). The CT images were obtained while patients were holding their breath, using the following parameters: tube voltage of 120 kV, tube current of 150–250 mA, section thickness of 5 mm, and reconstruction interval of 5 mm. An 80–100 mL dose of iohexol (General Electric Pharmaceuticals Shanghai Co., Ltd.) was administered at a rate of 5 mL/s via injection into an antecubital vein by high-pressure automatic injectors. The enhanced CT scans were performed in the renal corticomedullary phase (delayed 25–30 s), nephrographic phase (delayed 60–90 s), and excretory phase (delayed >20 min).

Image analysis

Another two radiologists with 10 and 20 years of experience, respectively, who were not involved in case selection, reviewed all selected cases in consensus on the picture archiving and communication system workstation. These two radiologists were blinded to the pathology results.

First, the two radiologists visually assessed the enhancement features of the central hypodense areas of these tumors. An enhancement inversion was considered to be present when the central hypodense areas enhanced slowly in a centripetal manner over time and showed higher attenuation than the peripheral tumor parenchyma in the excretory phase images. It was considered to be a complete enhancement inversion when the entire central hypodense areas were enhanced and showed higher attenuation and an incomplete enhancement inversion when only the periphery of the areas was enhanced and showed higher attenuation.

Second, the two radiologists selected the areas that demonstrated the maximum enhancement of the tumor in the corticomedullary phase images. Matching elliptical or round regions of interest (ROIs), approximately 8–15 mm^2 in size, were drawn in the same location in each of the three contrast-enhanced imaging phases. For each contrast-enhanced phase, two measurements of the same configuration and size were acquired on each lesion using a cursor, and the average value was recorded. Another ROI of the same size was drawn in the adjacent renal cortex to normalize variations in attenuation due to technical and individual factors. The ratio of lesion to cortex attenuation (L/C) was calculated using the formula (lesion ROI / cortex ROI) × 100%. In addition, the formula (lesion ROI$_{corticomedullary}$ − lesion ROI$_{nephrographic}$) was used to calculate absolute de-enhancement.

Pathologic findings were used as the gold standard.

Statistical analysis

Statistical analysis was conducted using SPSS for Windows software (ver. 25.0; IBM Inc.). Descriptive analyses used the mean and standard deviation (SD) for normally distributed numeric variables, median (min–max) values for non-normally distributed numeric variables, and n (%) for categoric variables. The enhancement inversion was compared between oncocytomas and ccRCCs using the Pearson chi-square test.

Main points

- A longer delay scanning time is valuable for distinguishing oncocytomas with a central scar from clear cell renal cell carcinomas (ccRCCs).

- The absence of enhancement inversion of the central hypodense areas in the excretory phase could be used to rule out oncocytoma.

- Quantitative analysis of the peripheral tumor parenchyma using the ratio of lesion to cortex attenuation in the corticomedullary phase and absolute de-enhancement showed significant value in differentiating oncocytomas from ccRCCs, but there were some overlaps.

- The combination of enhancement analysis of the central hypodense areas and peripheral tumor parenchyma provided high diagnostic specificity and negative predictive value.

The L/C and absolute de-enhancement were compared between oncocytomas and ccRCCs using the Student's t-test if normal distribution was achieved; otherwise, the non-parametric Mann–Whitney U test was used. The Kolmogorov–Smirnov test was used to evaluate the normality of quantitative data. A P value of <0.050 was considered to indicate a significant difference. Optimal cutoff values of L/C in the corticomedullary phase and absolute de-enhancement for identifying oncocytomas and ccRCCs were derived using receiver operating characteristic (ROC) curve analysis. To assess the diagnostic performance of these parameters for distinguishing oncocytomas from ccRCCs, accuracy, sensitivity, specificity, positive predictive value (PPV), and negative predictive value (NPV) were calculated.

Results

The study population consisted of 44 men (54.32%) and 37 women (45.68%); the median (min–max) age was 60 (37–83) years. All patients underwent partial or total nephrectomy, and data on postoperative histological diagnosis were obtained. The mean size ± SD of oncocytomas and ccRCCs was 4.8 ± 2.2 and 4.9 ± 1.5 cm, respectively.

The enhancement inversion analysis of the central hypodense areas is shown in Table 1. The central hypodense areas of all tumors showed either slow enhancement in a centripetal manner over time and enhancement inversion or no enhancement, which was observed in 72 (88.89%) and 9 (11.11%) cases, respectively. A complete enhancement inversion was observed in 28 (34.57%) cases, and in all cases, it was observed in the excretory phase (Figures 1, 2). An incomplete enhancement inversion was observed in 44 (54.32%) cases (Figures 3, 4). Complete enhancement inversion was more common in oncocytomas than in ccRCCs (P = 0.003).

Results of the enhancement analysis of the peripheral parenchyma of tumors are shown in Table 2 and Figure 5. The L/C in the corticomedullary phase significantly differed between oncocytomas and ccRCCs (P < 0.001);

in the nephrographic and excretory phases, the L/C overlapped considerably between oncocytomas and ccRCCs (P = 0.533 and P = 0.794, respectively). Oncocytomas had a significantly lower absolute de-enhancement than ccRCCs (P < 0.001). Optimal cut-off values of the L/C in the corticomedullary phase of 1.0 and absolute de-enhancement of 42.5 HU were extracted using ROC curve analysis (Figure 6) for identifying oncocytomas and ccRCCs. These values suggest that a tumor with an L/C in the corticomedullary phase lower than 1.0 or absolute de-enhancement lower than 42.5 HU can be considered as an oncocytoma.

The accuracy, sensitivity, specificity, PPV, and NPV obtained by different parameters are shown in Table 3. The combination of complete enhancement inversion and the quantitative features of peripheral tumor parenchyma provided high specificity and NPV for distinguishing oncocytomas from ccRCCs.

Discussion

The quantitative analysis of peripheral tumor parenchyma using the L/C in the corticomedullary phase and absolute de-enhancement showed significant value in identifying oncocytomas and ccRCCs, but there were some overlaps. The combination of enhancement features of central hypodense areas and peripheral tumor parenchyma provided high diagnostic specificity and NPV.

The central scar is an important radiological feature of oncocytomas, but it is not specific because the central necrosis that occurs within RCCs also shows hypodense areas on unenhanced CT, and the central scar also occurs in a small fraction of RCCs.[15] Moreover, the central scar does not always present a typical stellate pattern, making it more difficult to distinguish from irregular central necrosis within RCCs.[16] In our study, a longer delay scanning time (>20 min after injection) was used to evaluate the enhancement features of the central hypodense areas. Our study provides some important results. First, all oncocytomas presented complete or in-

complete enhancement inversion within the central hypodense areas in the excretory phase. This means that the absence of enhancement inversion of the central hypodense areas could be used to rule out oncocytoma. Second, complete enhancement inversion of the central areas was more common in oncocytomas than in ccRCCs. The difference may be related to different histopathologic structures of central areas in oncocytomas and ccRCCs.[1] Kim et al.[17] described the imaging feature of "segmental enhancement inversion" in homogeneous renal tumors smaller than 4 cm without a central scar; however, it is important to note that the segmental enhancement inversion was due to pathological differences in the stromal content within the tumor parenchyma, as opposed to the enhancement inversion of the central scar and peripheral tumor parenchyma in our study. Third, complete enhancement inversion was observed only in the excretory phase. This explains why it has never been mentioned with CT before, since a longer delay scanning time has not previously been used.[5,18]

Cornelis et al.[1] investigated the delayed enhancement features of central high T2-weighted signal intensity of oncocytomas and RCCs on MRI and first proposed the concept of enhancement inversion. In our study, the rate of complete enhancement inversion in ccRCCs was higher than that reported by Cornelis et al.[1] There are two possible explanations for this. First, we only included ccRCCs for our study, whereas the previous study included the three most common subtypes of RCCs. Second, in our study, the excretory phase images were obtained later than 20 min after contrast injection, whereas the late enhanced scanning was only carried out later than 5 min after contrast injection in the study by Cornelis et al.[1] We believe that a longer delay scanning time may result in a higher rate of complete enhancement inversion in ccRCCs. We speculate that there may be an optimal delay scanning time to better identify oncocytomas and ccRCCs based on enhancement features of the central hypodense areas, but solid evidence is needed to back this up.

The enhancement degree and pattern are valuable parameters for distinguishing oncocytoma from ccRCC.[19] Because there is no uniform standard, previous studies have used different measurement and enhancement correction methods, which has led to different and even completely opposing research results.[4,5,13,20,21] Wang et al.[22] reported that the degree of enhancement measured

Table 1. Enhancement analysis of the central hypodense areas of tumors

Enhancement of central hypodense areas	Type		P value
	Oncocytomas (n = 18)	ccRCCs (n = 63)	
None	0	9 (14.29%)	
Complete	12 (66.67%)	16 (25.40%)	0.003[a]
Incomplete	6 (33.33%)	38 (60.32%)	

[a], Pearson chi-square test; ccRCCs, clear cell renal cell carcinomas.
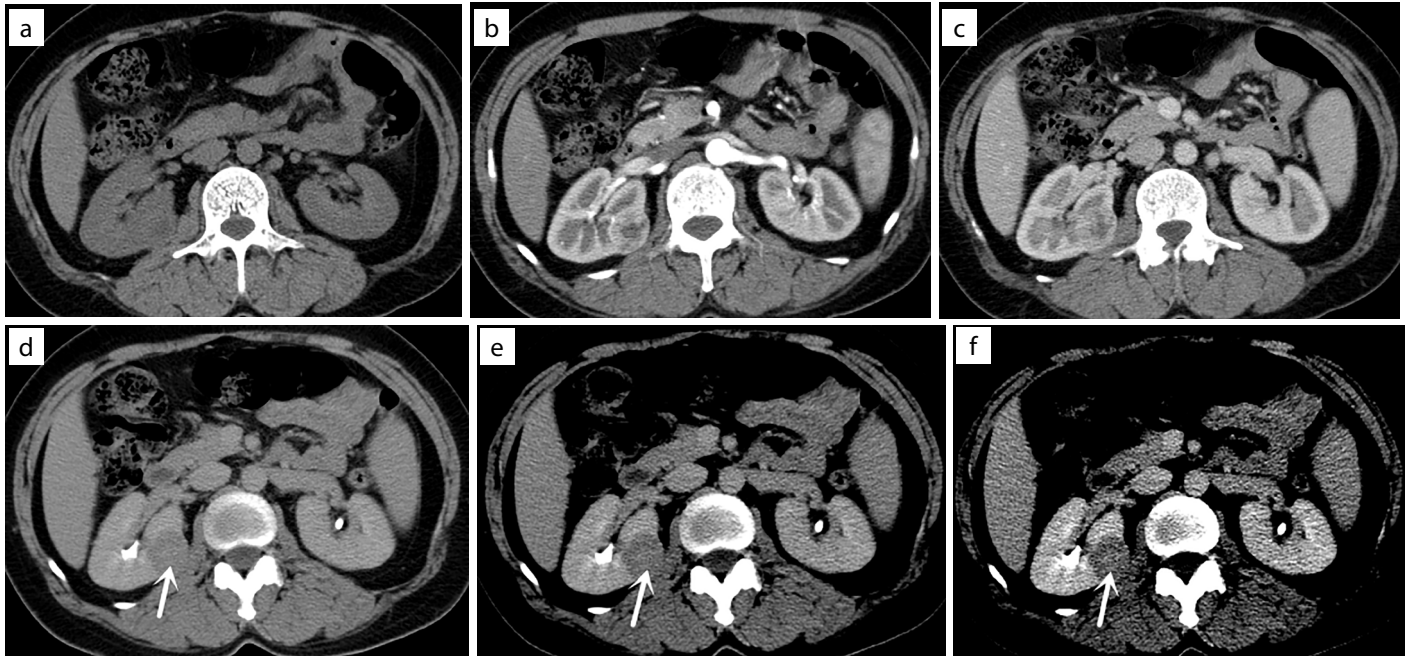
Figure 1. A 38-year-old woman with oncocytoma. **(a)** Axial unenhanced CT scan shows a 2.4 cm-diameter mass with central irregular hypodense areas. **(b-d)** Axial corticomedullary-, nephrographic-, and excretory-phase CT scans show that the central hypodense areas enhance slowly in a centripetal manner. The ratio of lesion to cortex attenuation in the corticomedullary phase and absolute de-enhancement are 0.66 and −44 HU, respectively. The excretory-phase CT scan shows that enhancement inversion is complete (arrow). **(e, f)** Axial excretory-phase CT scans with different windowing can better display the enhancement inversion of central hypodense areas (arrows). CT, computed tomography.
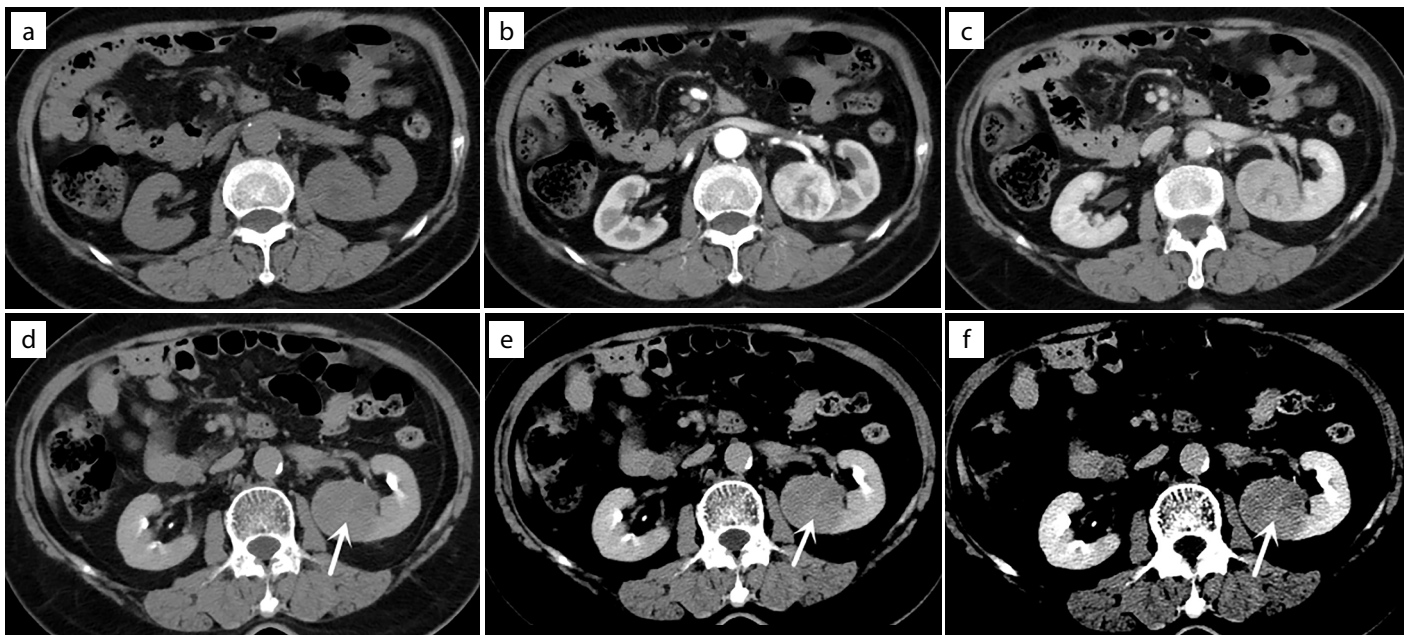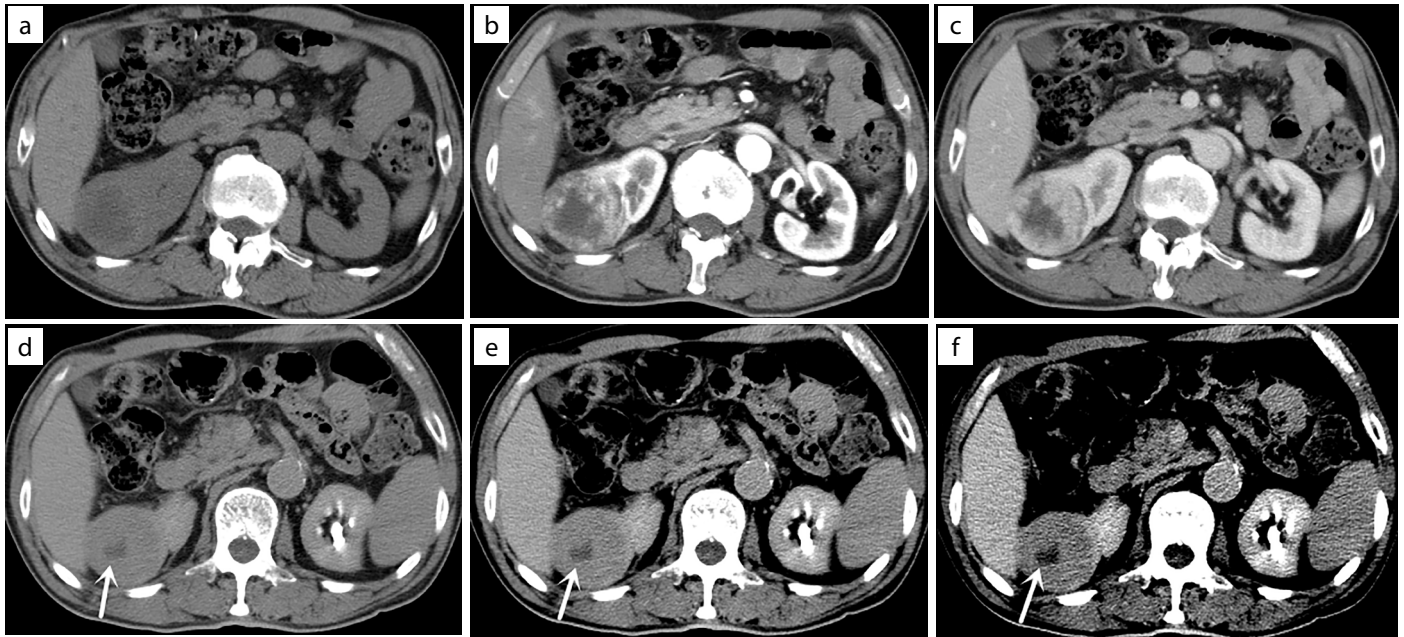

Figure 2. A 68-year-old woman with ccRCC. (**a**) Axial unenhanced CT scan shows a 3.9 cm-diameter mass with central irregular hypodense areas. **(b-d)** Axial corticomedullary-, nephrographic-, and excretory-phase CT scans show that the central hypodense areas appear slow with progressive enhancement in a centripetal manner. The ratio of lesion to cortex attenuation in the corticomedullary phase and absolute de-enhancement are 1.14 and 67 HU, respectively. The excretory-phase CT scan shows complete enhancement inversion of central areas (arrow). **(e, f)** Axial excretory-phase CT scans with different windowing can better display the complete enhancement inversion of central areas (arrows). ccRCC, clear cell renal cell carcinoma; CT, computed tomography.

using smaller ROIs (10–20 mm^2) performed better than small ROIs (50–100 mm^2) or large ROIs (included all components of the tumor on the largest cross-sectional images) for identifying renal angiomyolipoma without visible fat and small ccRCCs with CT. Therefore, in our study, we attempted to measure a smaller ROI (8–15 mm^2) to avoid the influ-ence of micronecrotic areas contained in ccRCCs and better reflect the enhancement degree of tumor. Our study showed that the L/C in the corticomedullary phase was significantly lower than the optimal cut-off value of 1.0 in nearly all oncocytomas (17/18, 94.44%) and higher than 1.0 in most ccRCCs (53/63, 84.13%). However, Bird et al.[21] meas-ured a larger ROI (100 mm^2) and reported that the L/C in the corticomedullary phase was highest for oncocytoma, followed by ccRCC. Gentili et al.[5] measured as large a tu-mor parenchyma as possible and concluded that oncocytomas are almost isodense and ccRCCs are mostly hypodense compared with the renal cortex in the corticomedul-

Figure 3. A 73-year-old man with oncocytoma. **(a)** Axial unenhanced CT scan shows a 4.9 cm-diameter mass with central irregular hypodense areas. **(b-d)** Axial corticomedullary-, nephrographic-, and excretory-phase CT scans show that the central hypodense areas enhance slowly in a centripetal manner except in the inner portion. The ratio of lesion to cortex attenuation in the corticomedullary phase and absolute de-enhancement are 0.62 and 15 HU, respectively. The excretory-phase CT scan shows that enhancement inversion appears incomplete. Note the higher enhancement at the junction between the central hypodense area and peripheral tumor component (arrow). **(e, f)** Axial excretory-phase CT scans with different windowing can better display the incomplete enhancement inversion of central areas (arrows). CT, computed tomography.
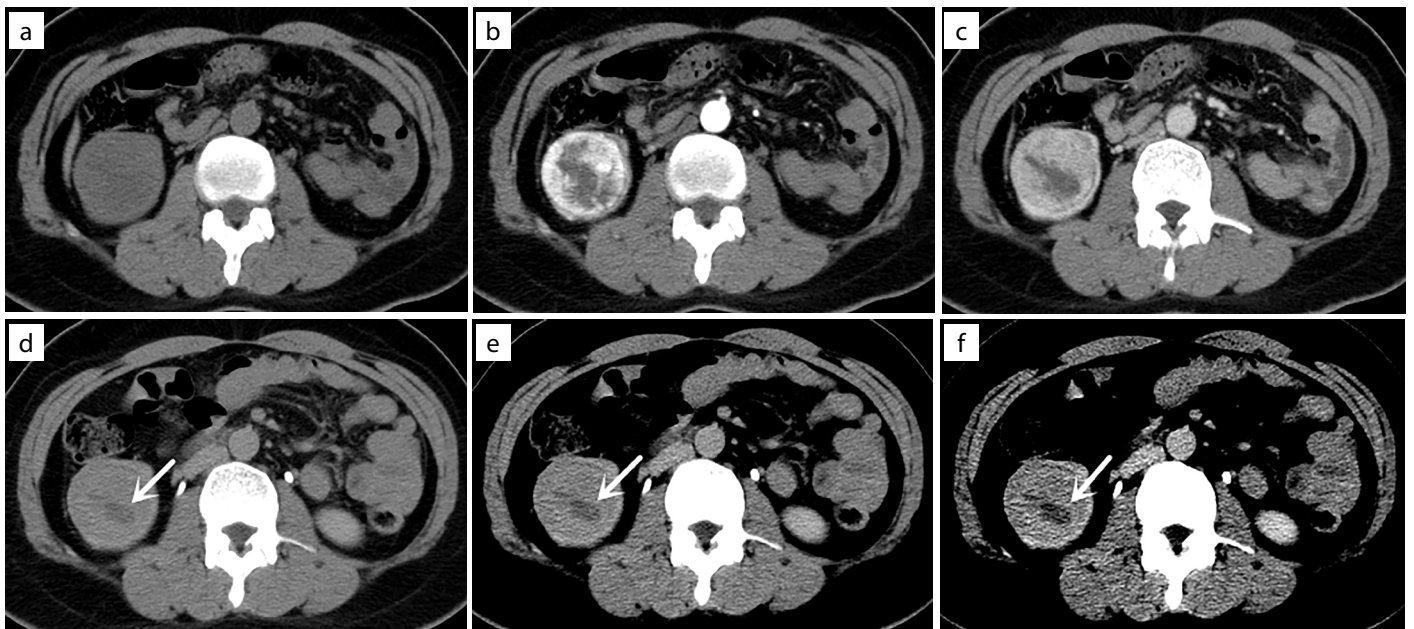
Figure 4. A 43-year-old woman with ccRCC. **(a, b)** Axial unenhanced and corticomedullary-phase CT scans show a 4.5 cm-diameter mass with central hypodense areas. The ratio of lesion to cortex attenuation in the corticomedullary phase is 1.23. **(c, d)** Axial nephrographic- and excretory-phase CT scans show that the central hypodense areas appear slow with progressive enhancement in a centripetal manner except in the inner portion. Absolute de-enhancement is 86 HU. The excretory-phase CT scan shows that enhancement inversion appears incomplete. Note the higher enhancement at the junction between the central hypodense areas and peripheral tumor component (arrow). **(e, f)** Axial excretory-phase CT scans with different windowing can better display the enhancement inversion of central hypodense areas (arrows). ccRCC, clear cell renal cell carcinoma; CT, computed tomography.

lary phase. Although Moldovanu et al.[23] also measured a smaller ROI (10 mm²) and found that oncocytoma had a higher enhancement change than ccRCC, the difference did not reach statistical significance. This suggests that different ROI sizes have a significant impact on the differentiation of oncocyto-ma from ccRCC. In our study, the L/C in the corticomedullary phase measured by smaller ROIs showed high sensitivity and NPV for differentiating oncocytoma from ccRCC. Some studies have found rapid washout enhance-ment pattern in ccRCCs on multiphase con-trast-enhanced CT.[4,12] Our study showed that absolute de-enhancement was significantly lower than the optimal cutoff value of 42.5 HU in most oncocytomas (15/18, 83.33%) and higher than 42.5 HU in most ccRCCs (50/63, 79.37%), similar to the finding of Lee-Felker et al.[13] Using the combination of L/C in the corticomedullary phase and absolute

Table 2. Enhancement analysis of the peripheral parenchyma of tumors

Enhancement of the tumor parenchyma	Type		P value
	Oncocytomas (n = 18)	ccRCCs (n = 63)	
L/C in the corticomedullary phase, median (min–max)	0.83 (0.62–1.06)	1.15 (0.47–2.01)	<0.001[a]
L/C in the nephrographic phase, mean ± SD	0.78 ± 0.12	0.76 ± 0.11	0.533[b]
L/C in the excretory phase, mean ± SD	0.71 ± 0.07	0.72 ± 0.16	0.794[b]
Absolute de-enhancement, median (min–max)	11 (−44–58)	67 (−12–220)	<0.001[a]

[a], Mann–Whitney U test; [b], Student's t-test; ccRCCs, clear cell renal cell carcinomas; L/C, ratio of lesion to cortex attenuation; SD, standard deviation.
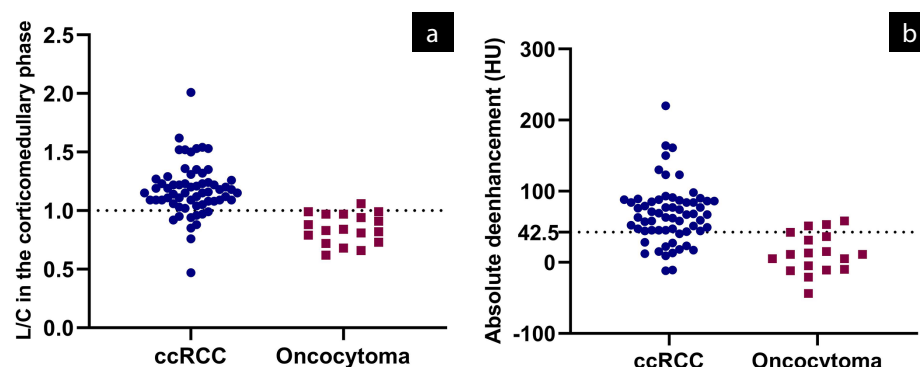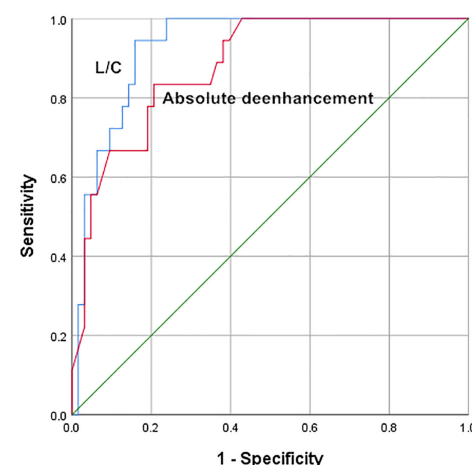

Figure 5. Scatterplots of the L/C in the corticomedullary phase and absolute de-enhancement for tumors of oncocytoma and ccRCC groups. (a) Scatterplot of the L/C in the corticomedullary phase. Most ccRCCs have an L/C higher than 1.0, whereas nearly all oncocytomas have a ratio lower than 1.0. (b) Scatterplot of absolute de-enhancement. Most ccRCCs have an absolute de-enhancement higher than 42.5 HU, whereas most oncocytomas have an absolute de-enhancement lower than 42.5 HU. L/C, ratio of lesion to cortex attenuation; ccRCC, clear cell renal cell carcinoma.

Figure 6. Receiver operating characteristic curve for the L/C in the corticomedullary phase and absolute de-enhancement for distinguishing oncocytomas from ccRCCs. The area under the receiver operating characteristic curve was 0.929 (95% CI, 0.874–0.983; SE, 0.028) for the L/C in the corticomedullary phase and 0.881 (95% CI, 0.802–0.959; SE, 0.040) for absolute de-enhancement. L/C, ratio of lesion to cortex attenuation; ccRCC, clear cell renal cell carcinoma; CI, confidence interval; SE, standard error.

Table 3. Accuracy of differentiation of oncocytomas from ccRCCs for all criteria

Criteria	Differentiation	Accuracy (%)	Sensitivity (%)	Specificity (%)	PPV (%)	NPV (%)
Enhancement inversion	Complete	72.84	66.67	74.60	42.86	88.68
	Incomplete	38.27	33.33	39.68	13.64	67.57
	Complete or incomplete	33.33	100.00	14.29	25.00	100.00
Enhancement of the peripheral tumor parenchyma	L/C in the corticomedullary phase ≤1.0	86.42	94.44	84.13	62.96	98.15
	Absolute de-enhancement ≤42.5 HU	80.25	83.33	79.37	53.57	94.34
	Combination of both criteria	90.12	83.33	92.06	75.00	95.08
Combination of both criteria	Complete enhancement inversion and L/C in the corticomedullary phase ≤1.0	86.42	61.11	93.65	73.33	89.39
	Complete enhancement inversion and absolute de-enhancement ≤42.5 HU	85.19	55.56	93.65	71.43	88.06
	Complete enhancement inversion and L/C in the corticomedullary phase ≤1.0 and absolute de-enhancement ≤42.5 HU	87.65	55.56	96.83	83.33	88.41

ccRCC, clear cell renal cell carcinoma; PPV, positive predictive value; NPV, negative predictive value; L/C, ratio of lesion to cortex attenuation.

de-enhancement was better than using a single parameter for distinguishing oncocytomas from ccRCCs. In conclusion, L/C in the corticomedullary phase or absolute de-enhancement provided a simple method that can be applied in the clinic for differential diagnosis. The two parameters can be used in combination to differentiate oncocytomas from ccRCCs.

Our study has some limitations. First, owing to the retrospective design, the analysis is subjected to some selection bias. Second, our study only evaluated tumors with central hypodense areas, which increased the rate of oncocytomas by excluding ccRCCs that were not associated with the typical central scar or necrosis. We did not evaluate oncocytomas or ccRCCs with a homogeneous appearance

or other subtypes of RCC. Third, although the two experienced radiologists reached a consensus when assessing the enhancement inversion, visual assessment could carry errors. Fourth, due to space constraints, we only chose simple and easy-to-operate measurement and enhancement correction methods; we did not compare the results with other measurement and enhancement correction

methods, and this might be an interesting future direction. Finally, because of the similar imaging features but different treatment strategies, most imaging studies on the differential diagnosis of benign and malignant renal tumors are based on the standard whose diameter are 4 cm or less. Though limiting the size of the lesions would add more value to our study, we did not do so because of the case number constraints.

In conclusion, a longer delay scanning time is valuable for distinguishing oncocytomas with a central scar from ccRCCs. Quantitative analysis of the peripheral tumor parenchyma showed some overlaps between oncocytomas and ccRCCs, and we provided optimal cutoff values. The addition of enhancement features of the central hypodense areas can provide high diagnostic specificity and NPV.

Conflict of interest disclosure

The authors declared no conflicts of interest.

References

1. Cornelis F, Lasserre AS, Tourdias T, et al. Combined late gadolinium-enhanced and double-echo chemical-shift MRI help to differentiate renal oncocytomas with high central T2 signal intensity from renal cell carcinomas. *AJR Am J Roentgenol.* 2013;200(4):830-838. [CrossRef]

2. Meagher MF, Lane BR, Capitanio U, et al. Comparison of renal functional outcomes of active surveillance and partial nephrectomy in the management of oncocytoma. *World J Urol.* 2021;39(4):1195-1201. [CrossRef]

3. Guo K, Ren S, Cao Y, et al. Differentiation between renal oncocytomas and chromophobe renal cell carcinomas using dynamic contrast-enhanced computed tomography. *Abdom Radiol (NY).* 2021;46(7):3309-3316. [CrossRef]

4. Ren A, Cai F, Shang YN, et al. Differentiation of renal oncocytoma and renal clear cell carcinoma using relative CT enhancement ratio. *Chin Med J (Engl).* 2015;128(2):175-179. [CrossRef]

5. Gentili F, Bronico I, Maestroni U, et al. Small renal masses (≤4 cm): differentiation of oncocytoma from renal clear cell carcinoma using ratio of lesion to cortex attenuation and aorta-lesion attenuation difference (ALAD) on contrast-enhanced CT. *Radiol Med.* 2020;125(12):1280-1287. [CrossRef]

6. Zhong Y, Wang H, Shen Y, et al. Diffusion-weighted imaging versus contrast-enhanced MR imaging for the differentiation of renal oncocytomas and chromophobe renal cell carcinomas. *Eur Radiol.* 2017;27(12):4913-4922. [CrossRef]

7. Akın IB, Altay C, Güler E, et al. Discrimination of oncocytoma and chromophobe renal cell carcinoma using MRI. *Diagn Interv Radiol.* 2019;25(1):5-13. [CrossRef]

8. Sasaguri K, Takahashi N. CT and MR imaging for solid renal mass characterization. *Eur J Radiol.* 2018;99:40-54. [CrossRef]

9. Grajo JR, Batra NV, Bozorgmehri S, et al. Validation of aorta-lesion-attenuation difference on preoperative contrast-enhanced computed tomography scan to differentiate between malignant and benign oncocytic renal tumors. *Abdom Radiol (NY).* 2021;46(7):3269-3279. [CrossRef]

10. Chen F, Gulati M, Hwang D, et al. Voxel-based whole-lesion enhancement parameters: a study of its clinical value in differentiating clear cell renal cell carcinoma from renal oncocytoma. *Abdom Radiol (NY).* 2017;42(2):552-560. [CrossRef]

11. Paño B, Soler A, Goldman DA, et al. Usefulness of multidetector computed tomography to differentiate between renal cell carcinoma and oncocytoma. A model validation. *Br J Radiol.* 2020;93(1115):20200064. [CrossRef]

12. Zokalj I, Marotti M, Kolarić B. Pretreatment differentiation of renal cell carcinoma subtypes by CT: the influence of different tumor enhancement measurement approaches. *Int Urol Nephrol.* 2014;46(6):1089-1100. [CrossRef]

13. Lee-Felker SA, Felker ER, Tan N, et al. Qualitative and quantitative MDCT features for differentiating clear cell renal cell carcinoma from other solid renal cortical masses. *AJR Am J Roentgenol.* 2014;203(5):W516-W524. [CrossRef]

14. Grajo JR, Terry RS, Ruoss J, et al. Using aorta-lesion-attenuation difference on preoperative contrast-enhanced computed tomography scan to differentiate between malignant and benign renal tumors. *Urology.* 2019;125:123-130. [CrossRef]

15. Giambelluca D, Pellegrino S, Midiri M, Salvaggio G. The "central stellate scar" sign in renal oncocytoma. *Abdom Radiol (NY).* 2019;44(5):1942-1943. [CrossRef]

16. Choudhary S, Rajesh A, Mayer NJ, Mulcahy KA, Haroon A. Renal oncocytoma: CT features cannot reliably distinguish oncocytoma from other renal neoplasms. *Clin Radiol.* 2009;64(5):517-522. [CrossRef]

17. Kim JI, Cho JY, Moon KC, Lee HJ, Kim SH. Segmental enhancement inversion at biphasic multidetector CT: characteristic finding of small renal oncocytoma. *Radiology.* 2009;252(2):441-448. [CrossRef]

18. Li X, Nie P, Zhang J, Hou F, Ma Q, Cui J. Differential diagnosis of renal oncocytoma and chromophobe renal cell carcinoma using CT features: a central scar-matched retrospective study. *Acta Radiol.* 2022;63(2):253-260. [CrossRef]

19. Allgood E, Raman SS. Image interpretation: practical triage of benign from malignant renal masses. *Radiol Clin North Am.* 2020;58(5):875-884. [CrossRef]

20. Kahn AE, Lomax SJ, Bajalia EM, Ball CT, Thiel DD. Utility of the aortic-lesion-attenuation-difference (ALAD) and peak early-phase enhancement ratio (PEER) to differentiate benign from malignant renal masses. *Can J Urol.* 2020;27(4):10278-10284. [CrossRef]

21. Bird VG, Kanagarajah P, Morillo G, et al. Differentiation of oncocytoma and renal cell carcinoma in small renal masses (<4 cm): the role of 4-phase computerized tomography. *World J Urol.* 2011;29(6):787-792. [CrossRef]

22. Wang X, Song G, Jiang H. Differentiation of renal angiomyolipoma without visible fat from small clear cell renal cell carcinoma by using specific region of interest on contrast-enhanced CT: a new combination of quantitative tools. *Cancer Imaging.* 2021;21(1):47. [CrossRef]

23. Moldovanu CG, Petresc B, Lebovici A, et al. Differentiation of clear cell renal cell carcinoma from other renal cell carcinoma subtypes and benign oncocytoma using quantitative MDCT enhancement parameters. *Medicina* (Kaunas). 2020;56(11):569. [CrossRef]